Dynamic model of epitaxial growth in ternary III-V semiconductor alloys

doi: 10.1103/PhysRevB.51.7104

Dynamic model of epitaxial growth in ternary III-V semiconductor alloys

Bing-Lin Gu
Department of Physics, Tsinghua University, Beijing 100084, People's Republic of China;
Center of Theoretical Physics, Chinese Center of Advanced Science and Technology (World Laboratory),
P.O. Box 8730, Beijing 100080, People's Republic of China;
and Institute for Materials Research, Tohoku University, Sendai 980, Japan

Zhi-Feng Huang
Department of Physics, Tsinghua University, Beijing 100084, People's Republic of China

Jun Ni
Department of Physics, Tsinghua University, Beijing 100084, People's Republic of China
and Center of Theoretical Physics, Chinese Center of Advanced Science and Technology (World Laboratory),
P.O. Box 8730, Beijing 100080, People's Republic of China

Jing-Zhi Yu, Kaoru Ohno, and Yoshiyuki Kawazoe
Institute for Materials Research, Tohoku University, Sendai 980, Japan
(Received 21 April 1994; revised manuscript received 20 October 1994)

A concentration-wave method for several interpenetrating Bravais sublattices is presented by considering the intralayer and interlayer effective interactions and the difference between the surface layers and the deep layers of ternary III-V alloys. The most stable ordered structures of ternary III-V semiconductor alloys are deduced and a dynamic model for epitaxial growth is proposed. The present results are compared with the experimental observations, and the relations between interaction parameters are also given.

I. INTRODUCTION

The long-range-ordered structures of III-V ternary semiconductor alloys in epitaxial growth have attracted much attention. There have been some experimental results[1–9] showing the $L1_1$ (CuPt-like) superstructure[2–7] (only two directions $[\bar{1}11]$ and $[1\bar{1}1]$ out of four possible directions have been found) and the coexistence of $[001]L1_0$, $[010]L1_0$, and $E1_1$ structures appear most commonly in (001) substrate growth.[8] In (110) substrate growth, only the [001] variant of the $L1_0$ structure has been reported.[1,9]

In theoretical research, total-energy calculations from first principles of the ordered structures have been conducted.[10–13] Initially, the stability of ordered structures was determined by bulk-structure calculations.[10] Many authors also considered the surface effect,[11] and CuPt ordering at the (001) surface was investigated for the Ga-In-P alloy in which the atomic mobilities and surface reconstruction was taken into account.[12] Recently, starting from surface thermodynamics, Osório *et al.*[13] used first-principles total-energy calculations for the surface and subsurface layers and the cluster-variation method to study the ground-state ordered structures and finite-temperature thermodynamics. They attributed the observed ordering features to a thermodynamically stable phase at the growth temperature.

Some pheonomenological models were applied to study the ordered structures. By means of the concentration-wave method,[14,15] Binglin Gu and Jun Ni[16] determined the most stable ordered structures for bulk alloys. Furthermore, based on a two-dimensional planar model, Jun Ni *et al.*[17] deduced the planar most stable ordered structures of a specific growth plane and obtained the possible ordered structures for the alloy through layer-by-layer growth process, but they considered only the interactions within a single growth plane. It has been shown[13] that because of the coupling between different growth layers, it was insufficient to determine the stacking process from two-dimensional planar structures to correct three-dimensional bulk structure by only considering a single layer. Therefore, the present study focuses on the interlayer effective interactions between different layers and also the intralayer interactions within a single growth plane. Accordingly, a phenomenological epitaxial growth model for ternary III-V alloys can be established.

We consider that the intralayer and interlayer effective interactions of the alloy are the main factors of the appearance of ordered structures, and surface layers and deep layers are different on structure stability in the layer-by-layer growth process of III-V alloys. Therefore, we apply the concentration wave method[14,15] for several interpenetrating Bravais sublattices to deduce the ordered structures. As is well known, each growth layer represents a planar Bravais lattice. If we want to consider the interlayer interactions to the third neighborhood, three consecutive growth layers must be included

and studied as a whole when we regard them as three interpenetrating planes. That is, three two-dimensional growth planes which are parallel to the substrate are considered as three interpenetrating Bravais lattices, and each plane represents a Bravais sublattice. Accordingly, we can get a quasi-two-dimensional lattice with a basis, and each basis consists of three atoms each belonging to a single growth plane. Therefore, we can simplify a three-dimensional problem to a quasi-two-dimensional one, and establish a model of epitaxial growth in the alloys to deduce the most stable ordered configurations. This method can be characterized as a three-interpenetrating-planes method.

The disordered phase structure in the ternary alloys of type $A^{\rm III}_{1-x}B^{\rm III}_{x}C^{\rm V}$ and $A^{\rm III}C^{\rm V}_{1-x}D^{\rm V}_{x}$ is zinc blende (Fig. 1). To simplify the contents, we consider the discussion only on the "common-cation" alloy $A^{\rm III}_{1-x}B^{\rm III}_{x}C^{\rm V}$ in the following deduction, which is applicable to "common anion" alloy $A^{\rm III}C^{\rm V}_{1-x}D^{\rm V}_{x}$. For the alloy $A^{\rm III}_{1-x}B^{\rm III}_{x}C^{\rm V}$ in an ordered phase, V atoms fully occupy one set of fcc positions, and $A^{\rm III}$, $B^{\rm III}$ atoms orderly occupy the other set, while in disordered phase $A^{\rm III}$ and $B^{\rm III}$ occupy randomly. Because the ordered structures all involve the ordering of the fcc positions occupied by III atoms, we consider only the planes occupied by atoms $A^{\rm III}$ and $B^{\rm III}$ in the three-interpenetrating-planes method.

In Sec. II, we describe the concentration-wave method for serveral interpenetrating Bravais sublattices. Formulation of a dynamic growth model and the ordered structures deduced from the model in (001), (110), and (111) substrate growth are given in Sec. III. Finally, we give the conclusion and compare the results to the experimental features.

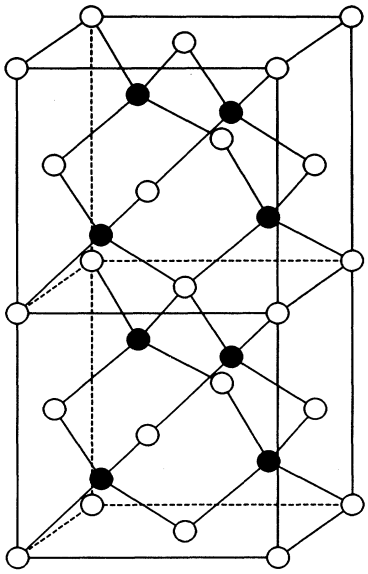

FIG. 1. The disorder structure of III-V ternary semiconductor $A^{\rm III}$-$B^{\rm III}$-$C^{\rm V}$, which is a zinc blende structure.

II. THE CONCENTRATION-WAVE THEORY

For several interpenetrating Bravais sublattices, the site vector of an atom is represented by

$$\mathbf{R}_\alpha = \mathbf{R} + \mathbf{h}_\alpha, \tag{2.1}$$

where $\mathbf{R}$ is the position vector of a unit cell and $\mathbf{h}_\alpha$ is the displacement of the αth sublattice with respect to the origin.

In the pair interaction approximation, the energy of the structure can be written as[15]

$$E = U_0 - \frac{N_A}{2}\sum_{\alpha\beta}\sum_{\mathbf{R}}{}'W_{\alpha\beta}(\mathbf{R}) + \frac{1}{2}\sum_{\alpha\beta}\sum_{\mathbf{R}\mathbf{R}'}{}'W_{\alpha\beta}(\mathbf{R}-\mathbf{R}')p(\alpha,\mathbf{R})p(\beta,\mathbf{R}'), \tag{2.2}$$

where

$$W_{\alpha\beta}(\mathbf{R}-\mathbf{R}') = W^{\alpha\beta}_{AA}(\mathbf{R}-\mathbf{R}') + W^{\alpha\beta}_{BB}(\mathbf{R}-\mathbf{R}') - 2W^{\alpha\beta}_{AB}(\mathbf{R}-\mathbf{R}'), \tag{2.3}$$

$$U_0 = \frac{N_A}{2}\sum_{\alpha\beta}\sum_{\mathbf{R}}{}' W^{\alpha\beta}_{AA}(\mathbf{R}) + \frac{N_B}{2}\sum_{\alpha\beta}\sum_{\mathbf{R}}{}' W^{\alpha\beta}_{BB}(\mathbf{R}), \tag{2.4}$$

and $W^{\alpha\beta}_{ij}(\mathbf{R}-\mathbf{R}')$ represents the effective interaction energy between ith ion at the $\mathbf{R}$ site in the αth sublattice and jth ion at the $\mathbf{R}'$ site in the βth sublattice. N_A and N_B are the numbers of A and B atoms, respectively. $\sum'$ means that the term for $\mathbf{R}$=$\mathbf{R}'$ is excluded in the sum. $p(\alpha,\mathbf{R})$ represents the occupation probability of A atom at $\mathbf{R}$ site in the αth sublattice.

After a Fourier transformation, Eq. (2.2) is transformed into a standard quadratic form,

$$E = U_0 - \frac{x(1-x)}{2}N\sum_{\alpha\beta}V_{\alpha\beta}(0) + \frac{N}{2}\sum_{\sigma}\sum_{\mathbf{k}}\lambda_\sigma(\mathbf{k})|Q_\sigma(\mathbf{k})|^2, \tag{2.5}$$

where

$$V_{\alpha\beta}(\mathbf{k}) = \sum_{\mathbf{R}}{}' W_{\alpha\beta}(\mathbf{R})\exp(i\mathbf{k}\cdot\mathbf{R}), \tag{2.6}$$

$$\sum_{\beta}V_{\alpha\beta}(\mathbf{k})\nu_\sigma(\beta,\mathbf{k}) = \lambda_\sigma(\mathbf{k})\nu_\sigma(\alpha,\mathbf{k}), \tag{2.7}$$

$\lambda_\sigma(\mathbf{k})$ and $\nu_\sigma(\alpha,\mathbf{k})$ are the eigenvalues and the orthonormal eigenvectors of $V_{\alpha\beta}(\mathbf{k})$, respectively. N is the sum of N_A and N_B.

Accordingly, $p(\alpha,\mathbf{R})$ is represented by

$$p(\alpha,\mathbf{R}) = x + \frac{1}{2}\sum_{\sigma}\sum_{\mathbf{k}}[\nu_\sigma(\alpha,\mathbf{k})Q_\sigma(\mathbf{k}) \times\exp(i\mathbf{k}\cdot\mathbf{R}) + \text{c.c.}], \tag{2.8}$$

where $Q_\sigma(\mathbf{k})$ are the amplitudes of the concentration wave and the corresponding normal concentration modes, x is the composition of A atoms.

The configurational energy in Eq. (2.5) derived for the pair interactions approximation has a form suitable for the instability analysis. It has been demonstrated[14,15,18] that instability will occur for the wave vectors $\mathbf{k}$ which will provide the absolute minimum of $\lambda_\sigma(\mathbf{k})$, and the structures of the most stable ordered phase are determined by these wave vectors. In detail, if $\lambda_\sigma(\mathbf{k}) > 0$, the energy reaches its minimum when all $Q_\sigma(\mathbf{k} \neq 0) = 0$, because any $Q_\sigma(\mathbf{k})$ which is not equal to zero will make the energy described by Eq. (2.5) increase. Therefore we have $p(\alpha, \mathbf{R}) = x$ from Eq. (2.8), which corresponds to the disordered state. If $\lambda_\sigma(\mathbf{k}) \leq 0$, in order to minimize the energy, the spectrum of the normal mode will tend to peak, that is, $Q_\sigma(\mathbf{k})$ will be its maximum, at those wave vectors $\mathbf{k}$ where $\lambda_\sigma(\mathbf{k})$ is minimum. Therefore in the pairwise interaction approximation, the necessary extremum condition for finding the absolute minimum of $\lambda_\sigma(\mathbf{k})$ in order to minimize the energy is given by[14,15,18,19]

$$\frac{\partial \lambda_\sigma(\mathbf{k})}{\partial \mathbf{k}}\Big|_{\mathbf{k}=\mathbf{k}_0} = 0 \qquad \text{and} \qquad \lambda_\sigma(\mathbf{k}_0) \leq 0. \tag{2.9}$$

If $\mathbf{k}_0 \neq 0$ and are the minimum points of $\lambda_\sigma(\mathbf{k})$, the most stable ordered structure appears.

In the first Brillouin zone, there are two kinds of $\lambda_\sigma(\mathbf{k})$ minima. The first kind corresponds to arbitrary points of the reciprocal space. Their positions depend on the type of interatomic interaction parameters, and they shift when the latter changes. The second kind is the high symmetry points (special points) according to the Lifshitz criterion,[20] which depend solely on the symmetry of the crystal disordered phase. At the special points, $\lambda_\sigma(\mathbf{k})$ must present extrema regardless of the choice of pair interaction, and the minima lead to the most stable ordered structures.

It is known that structure instabilities may occur for any position $\mathbf{k}$ in reciprocal space. However, as has been pointed out by Sanchez, Gratias, and Fontaine,[18] special-point ordered structures have the smallest Bravais lattice compatible with the disordered phase, and will invariably be ground states for short-range interactions.

It must be noticed that the configurational energy in Eq. (2.2) is presented in the pairwise interaction approximation, and what we discuss above corresponds to the case when only the harmonic terms of the configurational free energy is considered, which has been generally discussed.[14,18,19] When the anharmonic contributions are included, the stability of the ordered structures is thus due not to a minimum of $\lambda_\sigma(\mathbf{k})$, that is, Eq. (2.9) is not true in this case. Therefore the wave vectors $\mathbf{k}_0$, which minimize the energy, can deviate from special points.[18]

To study the epitaxial growth mechanism of ternary III-V alloys, we consider that the properties of the alloys are governed mainly by the harmonic part, and the anharmonic contributions can be neglected. In our three-interpenetrating-planes methods only the limited range of intralayer and interlayer effective pair interactions to the third neighborhood are included, and the long-range interactions are neglected. Then in the present case, the most stable ordered crystalline structures are determined by the special points in the first Brillouin zone.

For the special points in the first Brillouin zone, all the wave vectors $\mathbf{k}$, which make E minimum in the same star are denoted by s, and j_s refer to different wave vectors belonging to the same star $\{\mathbf{k}_{j_s}\}$. $\eta_{s\sigma}$ represents the long-range order parameter, and $\gamma_{s\sigma}$ is the coefficient related to the symmetry. The explicit expression of $p(\alpha, \mathbf{R})$ is

$$p(\alpha, \mathbf{R}) = x + \frac{1}{2}\sum_s \sum_\sigma \eta_{s\sigma} \times \sum_{j_s} [\gamma_{s\sigma}(j_s)\nu_\sigma(\alpha, \mathbf{k}_{j_s})\exp(i\mathbf{k}_{j_s} \cdot \mathbf{R}) + \text{c.c.}]. \tag{2.10}$$

We consider the most stable structure which is a complete ordered phase, and $\eta_{s\sigma} = 1$. To solve Eq. (2.10), we first set $\eta_{s\sigma} = 1$, and all the solutions of equation $p(\alpha, \mathbf{R}) = 0$ or 1 are just the most stable structures.

III. A GROWTH MODEL AND ORDERED STRUCTURES

In the following, we will establish a model of ternary III-V alloys in epitaxial growth by the "three-interpenetrating-planes method," and the growth on (001), (110), and (111) substrate will be considered. We specify three consecutive growth layers of the alloy which are parallel to the substrate as three interpenetrating Bravais sublattices, and each Bravais sublattice represents a layer. So the lattice with a basis, which consists of the atoms of three layers is formed, and there are three atoms per unit cell. Therefore, according to this interpenetrating method, the effective interactions between different layers can be considered. Figure 2 shows the structure of the alloy in (001) substrate growth. The corresponding high symmetry points and the first Brillouin

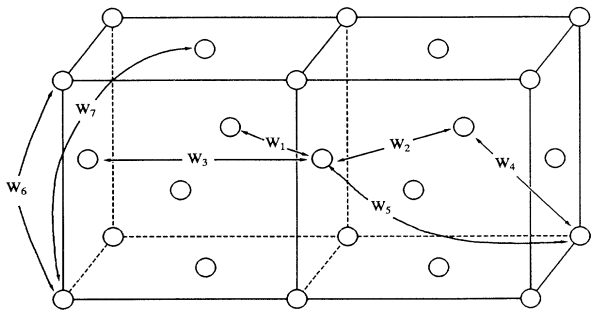

FIG. 2. The structure of the alloy in (001) substrate growth (only the sites occupied by A^{III} and B^{III} atoms are shown). W_1, W_2, W_3 represent the intralayer interaction parameters in each plane. The interlayer interactions between first-neighbor layers are W_4 and W_5, respectively. W_6 and W_7 denote the interlayer interactions between second-neighbor layers in the alloy.

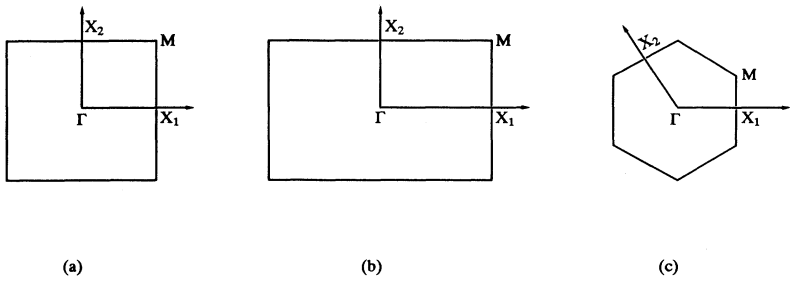

FIG. 3. First Brillouin zones and the corresponding high symmetry points for the single growth plane. (a) (001) plane, (b) (110) plane, (c) (111) plane.

zones in the (001), (110), and (111) substrate growth are shown in Figs. 3(a), (b), and (c), respectively.

A. Growth model

In expitaxial growth, the alloy grows layer-by-layer on a substrate. Figure 4 shows the growth process, where layers 0,2,4,6,... refer to the growth planes occupied by A^{III} and B^{III} atoms. Layers 1,3,5,..., occupied by C^{V} atoms are omitted in the figure because layers 1,3,5..., are the fcc positions fully occupied by V group atoms, and ordering only occurs among the positions occupied by A^{III} and B^{III}, that is, layers labeled by 0,2,4,.... Therefore, we consider only the ordering situation in layers 0,2,4,.... In the following discussion, we assume the three following conditions.

(i) In this model, we consider only the interactions among three consecutive growth layers. This model is schematically shown in Figs. 2(a), (b), and (c). The intralayer interactions in surface layers are different from those in deep layers. So do the interlayer interactions.

(ii) When the interlayer interactions to third neighborhood are considered, three consecutive growth layers are coupled to each other. During the growth process of the alloy, if a new layer is deposited above, it would influence the structures of top two layers. Because we neglect the fourth-neighbor interlayer interaction, the new layer will not couple to the third layer and below, whose structures are no longer changed accordingly. Therefore, the top two layers of the alloy are considered as surface layers, whose structures are not fixed and are subject to change with the cover of a new layer. However, further interior layers in the alloy which we call the deep layers are not influenced by the cover of the new layer, and their structures are stable. Therefore, these two kinds of layers must be treated differently. In Fig. 4 the layers with "d" are deep layers in the alloy, and the others are surface layers.

(iii) We consider that the controlled conditions during the whole epitaxial growth process of the alloy are no longer changed. Thus the intralayer and interlayer interaction relations of the alloy remain the same during the process.

Figures 4(a)–(f) show the growth process in detail. For instance, Fig. 4(d) is the case when the structure in Fig. 4(c) is covered by a new layer 4. Then this layer 4 affects the structures of layer 6 and 8 in Fig. 4(c) and changes them into the structure of layer 8 and the deep layer structure of layer 10 in Fig. 4(c), respectively. It has no influence on the deep layer structure of layer 10 in Fig. 4(d). From the process shown in Fig. 4, we can regard that the whole structures of the three top layers as a unit in Figs. 4(c)–(f) are invariant, where the top two are the surface layers and the third is of the deep layer structure which is the same as the inner layer structure in the alloy. So we only have to deduce the ordered structure of this three-top-layers unit. We can, therefore, stack layer by layer according to the growth process in Fig. 4. Finally, the whole ordered structure of the alloy is determined.

For this three-top-layers unit (just three-interpenetrating planes), $V_{00}(\mathbf{k}) \neq V_{22}(\mathbf{k}) \neq V_{44}(\mathbf{k}) \neq 0$, in general, where V_{00}, V_{22}, V_{44} are the intralayer interactions in the $\mathbf{k}$ space of the three top planes denoted by 0, 2, and 4 [see Eq. (2.6)]. Solving Eq. (2.7), one can find the ordered structures only if a high symmetry point $\mathbf{k}$

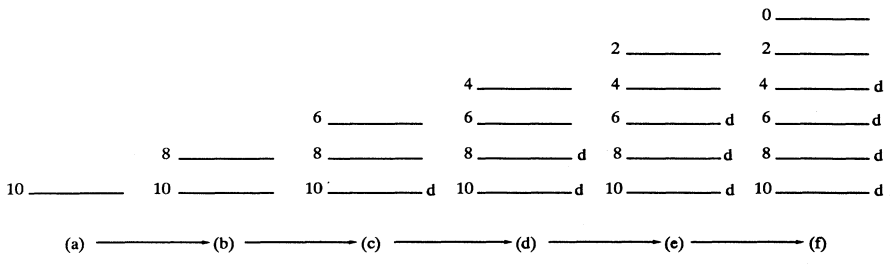

FIG. 4. The growth process of the III-V ternary semiconductor alloy. Layers 0, 2, 4, 6,... all refer to the growth planes occupied by A^{III} and B^{III} atoms, and layers 1, 3, 5,... that are occupied by V atoms are omitted. Layers with "d" are deep layers in the alloy, the others are surface layers. Then the layer-by-layer stacking process of the alloy is shown from (a) to (f).

satisfies the condition,

$$V_{02}(\mathbf{k}) = V_{24}(\mathbf{k}) = 0, \tag{3.1}$$

where V_{02} and V_{24} are the interlayer interactions in $\mathbf{k}$ space according to Eq. (2.6) between layers 0 and 2, 2, and 4, respectively. This condition seems to be very difficult to fulfill. But it can be seen below that for some high symmetry points, this condition can be satisfied, and the long-range ordered structures deduced from this condition agree with the experimental results. This condition implies that the coupling between first-neighbor layers occupied by atoms III is too small to be considered, which is also consistent with the first-principle calculations of Osório *et al.*[13]

(1) Degenerate case. When the energies corresponding to two high symmetry points, $\mathbf{k}_1$ and $\mathbf{k}_2$ belonging to different stars are degenerate, the ordered structure can be deduced. One of the high symmetry points, $\mathbf{k}_1$ must satisfy

$$V_{22} < \frac{1}{2}\left[(V_{00}+V_{44}) - \sqrt{(V_{00}-V_{44})^2 + 4V_{04}^2}\right], \tag{3.2}$$

then the eigenvalue is $\lambda_\sigma(\mathbf{k}_1) = V_{22}(\mathbf{k}_1)$, the eigenvector is $\nu_1 = (0,1,0)$.

The other high symmetry point $\mathbf{k}_2$ must satisfy

$$V_{00}(\mathbf{k}_2) = V_{44}(\mathbf{k}_2)$$

and

$$V_{00}(\mathbf{k}_2) - |V_{04}(\mathbf{k}_2)| < V_{22}(\mathbf{k}_2), \tag{3.3}$$

thus the eigenvalue is $\lambda_\sigma(\mathbf{k}_2) = V_{00}(\mathbf{k}_2) - |V_{04}(\mathbf{k}_2)|$, the eigenvector is $\nu_2 = (1,0,\pm 1)$.

Finally, as shown before, for both degenerate high symmetry points $\mathbf{k}_1$ and $\mathbf{k}_2$, we have

$$V_{02}(\mathbf{k}) = V_{24}(\mathbf{k}) = 0 \quad \text{and} \quad \lambda_\sigma(\mathbf{k}_1) = \lambda_\sigma(\mathbf{k}_2) \le 0. \tag{3.4}$$

(2) Undegenerate case. For certain high symmetry points $\mathbf{k}$, if the conditions

$$V_{00}(\mathbf{k}) = V_{44}(\mathbf{k})$$

and

$$V_{22}(\mathbf{k}) = V_{00}(\mathbf{k}) - |V_{04}(\mathbf{k})| \le 0 \tag{3.5}$$

are satisfied, the eigenvector ν is $(\pm 1, \pm 1, \pm 1)$. Therefore by this three-interpenetrating-planes method, the same two-dimensional ordered structures for each growth layer can be obtained. Accordingly, we can deduce the most stable ordered structures which are almost the same as the results based on the two-dimensional planar model presented by Jun Ni *et al.*[17] So it is unnecessary to solve the undegenerate case in detail here. In the following we only consider the degenerate case, and deduce the corresponding ordered structures.

B. Ordered structures

According to the three interaction relations Eqs. (3.2), (3.3), and (3.4) for the degenerate case, we will deduce the most stable ordered structures of three-top-layers unit in (001), (110), and (111) substrate growth and of the whole alloy after stacking layer by layer as shown in Fig. 4.

First, we calculate the case in (001) substrate growth in detail. W_1, W_2, W_3 represent the intralayer interaction parameters in each plane, where W_1 and W_2 are two different kinds of first-nearest neighbor interactions because of the existence of V atoms below the layer. The next-nearest neighbor interaction is denoted as W_3. W_4 and W_5 represent the interlayer interactions between first-neighbor layers. W_6 and W_7 denote the interlayer interactions between second-neighbor layers in an alloy (see Fig. 2). Accordingly from Eq. (2.6), for $\mathbf{k}(h,k)$, we obtain

$$\begin{aligned}
V_{00} &= 2W_1'\cos 2\pi h + 2W_2'\cos 2\pi k \\
&\quad +2W_3'[\cos 2\pi(h+k) + \cos 2\pi(h-k)], \\
V_{22} &= 2W_1''\cos 2\pi h + 2W_2''\cos 2\pi k \\
&\quad +2W_3''[\cos 2\pi(h+k) + \cos 2\pi(h-k)], \\
V_{44} &= 2W_1\cos 2\pi h + 2W_2\cos 2\pi k \\
&\quad +2W_3[\cos 2\pi(h+k) + \cos 2\pi(h-k)], \\
V_{02} = V_{20}^* &= 2W_4[\cos\pi(h-k) + \cos\pi(h+k)] \\
&\quad +2W_5[\cos\pi(h+3k) + \cos\pi(h-3k) \\
&\quad + \cos\pi(3h+k) + \cos\pi(3h-k)], \\
V_{24} = V_{42}^* &= 2W_4'[\cos\pi(h-k) + \cos\pi(h+k)] \\
&\quad +2W_5'[\cos\pi(h+3k) + \cos\pi(h-3k) \\
&\quad + \cos\pi(3h+k) + \cos\pi(3h-k)], \\
V_{04} = V_{40}^* &= W_6 + 2W_7[\cos 2\pi h + \cos 2\pi k].
\end{aligned} \tag{3.6}$$

For the high symmetry points $\Gamma(0,0)$, $X_1(\frac{1}{2},0)$,

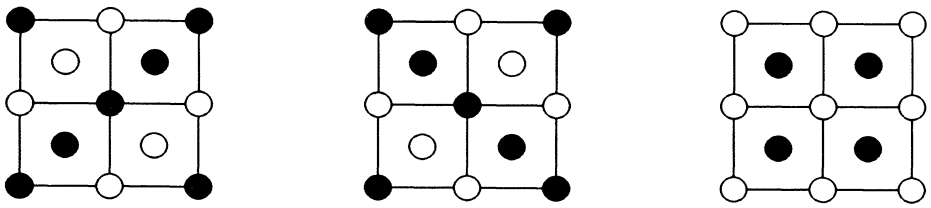

(a) O_1 (b) O_2 (c) O_3

FIG. 5. Two-dimensional planar ordered structures of (001) plane. (a) O_1, (b) O_2, (c) O_3.

TABLE I. All of the possible most stable ordered structures of III-V ternary semiconductor alloy according to the present growth model, where O_1, O_2, O_3, O_5, O_6, O_7, O_9, O_{10}, and O_{11} are the planar ordered structures shown in Figs. 5, 6, and 7, respectively. In the table, A represents A^{III} atom, and B represents B^{III} atom. The "whole alloy configuration" in the table consists of the structures of layers occupied by III atoms, where the leftmost structure is of the top layer.

Substrate	Ordered structure types	Whole alloy configuration
(001)	$\frac{1}{2}L1_1[\bar{1}11]$, $\frac{1}{2}L1_1[1\bar{1}1]$, $\frac{1}{2}[1\bar{1}0]$	$O_1O_2O_1O_1O_1\ldots$
		$O_1O_3O_1O_1O_1\ldots$
	$\frac{1}{2}L1_1[111]$, $\frac{1}{2}L1_1[11\bar{1}]$, $\frac{1}{2}[110]$	$O_2O_1O_2O_2O_2\ldots$
		$O_2O_3O_2O_2O_2\ldots$
	$L1_0[100]$, $L1_0[010]$, $\frac{1}{2}E1_1[021]$	$O_3O_1O_3O_3O_3\ldots$
		$O_3O_2O_3O_3O_3\ldots$
	$L1_0[001]$	$AO_5ABAB\ldots$
		$AO_6ABAB\ldots$
		$AO_7ABAB\ldots$
(110)	$\frac{1}{2}L1_1[111]$, $\frac{1}{2}L1_1[11\bar{1}]$, $\frac{1}{2}[001]$	$O_5AO_5O_5O_5\ldots$
		$O_5O_6O_5O_5O_5\ldots$
		$O_5O_7O_5O_5O_5\ldots$
	$L1_0[100]$, $L1_0[010]$, $\frac{1}{2}[1\bar{1}0]$	$O_6AO_6O_6O_6\ldots$
		$O_6O_5O_6O_6O_6\ldots$
		$O_6O_7O_6O_6O_6\ldots$
	$\frac{1}{2}L1_1[\bar{1}11]$, $\frac{1}{2}L1_1[1\bar{1}1]$, $\frac{1}{2}E1_1[021]$	$O_7AO_7O_7O_7\ldots$
		$O_7O_5O_7O_7O_7\ldots$
		$O_7O_6O_7O_7O_7\ldots$
(111)	$L1_0[001]$, $\frac{1}{2}L1_1[11\bar{1}]$	$O_9AO_9O_9O_9\ldots$
	$L1_0[100]$, $\frac{1}{2}L1_1[\bar{1}11]$	$O_{10}AO_{10}O_{10}O_{10}\ldots$
	$L1_0[010]$, $\frac{1}{2}L1_1[1\bar{1}1]$	$O_{11}AO_{11}O_{11}O_{11}\ldots$

$X_2(0,\frac{1}{2})$, and $M(\frac{1}{2},\frac{1}{2})$, from Eq. (3.6) we have $V_{02}(\Gamma)\neq 0$, $V_{24}(\Gamma)\neq 0$, and V_{02}, V_{24} for X_1, X_2, M points are all equal to zero. Then the condition Eq. (3.1) is fulfilled for X_1, X_2, and M, the ordered structures can be deduced by solving Eq. (2.7). According to Sec. III A, we only consider the degenerate case for X_1, X_2, M points.

When $X_1(\frac{1}{2},0)$ and $X_2(0,\frac{1}{2})$ are degenerate, we have the following.

(i) If X_1 satisfies relation Eq. (3.3), $V_{00}(X_1) = V_{44}(X_1)$, $\lambda_2(X_1) = V_{00} - |V_{04}|$, $\nu_2 = (1,0,\pm 1)$, and X_2 satisfies relation Eq. (3.2), $\lambda_1(X_2) = V_{22}(X_2)$, $\nu_1 = (0,1,0)$. Equation (2.10) gives

$p(0,\mathbf{R}) = x + \eta_{12}\gamma_{12}\cos\pi x$ for the first layer 0,
$p(2,\mathbf{R}) = x + \eta_{11}\gamma_{11}\cos\pi y$ for the second layer 2,
$p(4,\mathbf{R}) = x \pm \eta_{12}\gamma_{12}\cos\pi x$ for the third layer 4.

We get $x = 1/2$, $\gamma_{11} = \gamma_{12} = 1/2$. The corresponding ordered structure of the first layer and the third layer is denoted by O_1 [shown in Fig. 5(a)], and the structure of the second plane by O_2 [shown in Fig. 5(b)]. Then we have determined the ordered structure of the three-top-layers unit as $O_1O_2O_1$, which is consistent with the result of Osório *et al.*[13] According to the model shown in Sec. III A, we can stack the layers, and obtain the whole ordered structure configuration: $O_1O_2O_1O_1O_1\ldots$, where the deep layers have the same ordered structure $O_1O_1O_1\ldots$.

(ii) If X_1 satisfies Eq. (3.2) and X_2 satisfies Eq. (3.3), we can similarly get the ordered structure of the unit as $O_2O_1O_2$, and the whole ordered configuration as $O_2O_1O_2O_2O_2\ldots$.

Using the same process, we can obtain the ordered structure of the other cases which are degenerate between $X_1(\frac{1}{2},0)$ and $M(\frac{1}{2},\frac{1}{2})$, or $X_2(0,\frac{1}{2})$ and $M(\frac{1}{2},\frac{1}{2})$. The results are listed in Table I, where O_1, O_2, O_3 are the planar ordered structures shown in Figs. 5(a), (b), and (c).

If we assume that the deep layer structures of the alloy determine the long-range ordered structure, we can get the following.

Deep layers structure $O_1O_1O_1\ldots$ corresponds to the ordered structure $\frac{1}{2}[1\bar{1}1]L1_1$, $\frac{1}{2}[\bar{1}11]L1_1$, and $\frac{1}{2}[1\bar{1}0]$; structure $O_3O_3O_3\ldots$ corresponds to the ordered structure $[010]L1_0$, $[100]L1_0$, and $\frac{1}{2}[021]E1_1$; and $\frac{1}{2}[111]L1_1$, $\frac{1}{2}[11\bar{1}]L1_1$, and $\frac{1}{2}[110]$ are deduced by deep layers structure $O_2O_2O_2\ldots$.

The results of (110) and (111) substrates growth can be obtained by the same method. For brevity, we only list the results in Table I, where O_5, O_6, O_7 and O_9, O_{10}, O_{11} denote the planar ordered structures (Fig. 6, Fig. 7).

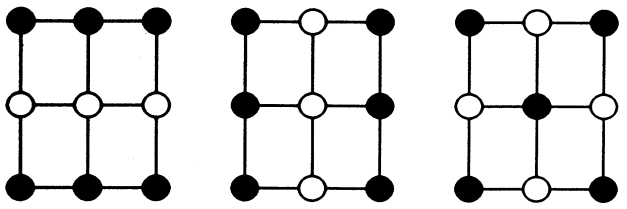

FIG. 6. Two-dimensional planar ordered structures of (110) plane. (a) O_5, (b) O_6, (c) O_7.

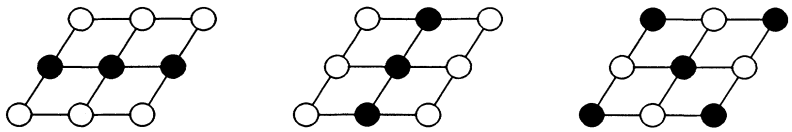

(a) O_9 (b) O_{10} (c) O_{11}

FIG. 7. Two-dimensional planar ordered structures of (111) plane. (a) O_9, (b) O_{10}, (c) O_{11}.

IV. CONCLUSION AND DISCUSSION

From the arguments given above, we arrive at the following conclusions from the proposed model of epitaxial growth.

(i) The surface layers in the alloy are considered as changeable, while the stable structures of deep layers determine the long-range ordered structures of the alloy. Then, we obtain the three-dimensional bulk ordered structures. If the *surface thermodynamics* is considered, according to Zunger and co-workers,[13,14] surface effects could lead to long-range ordering and the ordering is determined by the ordered phases of surface layers depending on atomic mobilities. Accordingly, the top layer couples to the layer 4 to select the three-dimensional ordered structures. It does not contradict our results. The results in Sec. III show that the planar structure of top layer 0 and layer 4 are the same through coupling, and are also the same as the deep layers structure. Therefore, the results both of the surface thermodynamics and deep layers stacking are consistent with each other. For instance, in Table I, the configuration $O_1O_2O_1O_1O_1O_1...$ leads to the CuPt structure according to both the surface structures[12,13,17] and the deep layers structures.

(ii) From the calculation in Sec. III, we have $V_{02} = V_{24} = 0$. Therefore, the coupling between first-neighbor layers can be omitted, which is in agreement with the results of Ref. 13. Accordingly, many possibilities appear during the stacking process of deep layers. Consequently, one ordered configuration of the deep layers lead to several kinds of ordered structures, such as the coexistence of $[100]L1_0$, $[010]L1_0$, and $\frac{1}{2}[021]E1_1$ according to the configuration of deep layers $O_3O_3O_3...$. This result is consistent with other works[13,17] and experiments.

(iii) The intralayer interactions and interlayer interactions in the alloy are the main factor of the appearance of ordered structures; different ordered structures appear because of the different interaction conditions.

(iv) If we want to determine the most stable ordered structures in the epitaxial growth of the actual alloy, the interaction relations, such as relations Eqs. (3.2), (3.3), and (3.4), should be used.

We have determined the possible most stable ordered structures of III-V ternary alloys for degenerate case, which are listed in Table I. The present results can explain some experimental phenomena in epitaxial growth. In (001) substrate growth, the coexistence of $L1_0$ and $E1_1$ structures, and especially the appearance of only two of three variants of $L1_0$ structure, can be explained by the configuration $O_3O_3O_3...$ of deep layers in Table I. The planar ordered structure O_1 of deep layers leads to the appearance of two variants of $L1_1$ structure, $\frac{1}{2}[1\bar{1}1]L1_1$, and $\frac{1}{2}[\bar{1}11]L1_1$, and the other two variants appear because of the planar structure O_2. From Sec. III, we can see that there are two different nearest-neighbor intralayer interaction parameters W_1 and W_2 due to the V atoms under the (001) plane, then the energies of O_1 and O_2 structures are different. Several previous calculations have shown that the O_1 structure is selected to meet the minimum energy of the alloy.[12,13]

The results about the (110) substrate growth in Table I are more complex, and the appearance of $[001]L1_0$ structure can be predicted. The other structures have not been found by the experiment. The ordered structure in (111) substrate growth has not been reported. Our results about it are just theoretical predictions, and the possible ordered structures are given in Table I. It may be noticed that to determine the possibility of the existence of these structures, the interaction relations [Eqs. (3.2), (3.3), and (3.4)] of each ordered structure should be used and be applied to the specific ternary III-V semiconductor alloys.

[1] T. S. Kuan, T. F. Kuech, W. I. Wang, and E. L. Wilkie, Phys. Rev. Lett. **54**, 201 (1985).

[2] W. E. Plano, D. W. Nam, J. S. Major, Jr., K. C. Hsieh, and N. Holonyak, Jr., Appl. Phys. Lett. **53**, 2537 (1988).

[3] P. Bellon, J. P. Chevalier, G. P. Martin, E. Dupont-Nivet, C. Thiebaut, and J. P. André, Appl. Phys. Lett. **52**, 567 (1988).

[4] G. B. Stringfellow and G. S. Chen, J. Vac. Sci. Technol. B **9**, 2182 (1991).

[5] Y. E. Ihm, N. Otsuka, J. Klem, and H. Morkoc, Appl. Phys. Lett. **51**, 2013 (1987).

[6] H. R. Jen, K. Y. Ma, and G. B. Stringfellow, Appl. Phys. Lett. **54**, 1154 (1989).

[7] H. R. Jen, D. S. Cao, and G. B. Stringfellow, Appl. Phys. Lett. **54**, 1890 (1989).

[8] H. R. Jen, M. J. Cherng, and G. B. Stringfellow, Appl. Phys. Lett. **48**, 1603 (1986).

[9] T. S. Kuan, W. I. Wang, and E. L. Wilkie, Appl. Phys. Lett. **51**, 51 (1987).

[10] G. P. Scrivastava, J. L. Martins, and A. Zunger, Phys. Rev. B **31**, 2561 (1985).

[11] S. Matsumura, N. Kuwano, and K. Oki, Jpn. J. Appl. Phys.

29, 688 (1990).
[12] S. Froyen and A. Zunger, Phys. Rev. Lett. **66**, 2132 (1991).
[13] R. Osório, J. E. Bernard, S. Froyen, and A. Zunger, Phys. Rev. B **45**, 11 173 (1992).
[14] A. G. Khachaturyan, Phys. Status Solidi B **60**, 90 (1973).
[15] Binglin Gu, Jun Ni, and Xiaowen Zhang, J. Appl. Phys. **70**, 4224 (1991).
[16] Binglin Gu and Jun Ni, J. Phys. Condens. Matter **4**, 9339 (1992).
[17] Jun Ni, Xinchun Lai, and Binglin Gu, J. Appl. Phys. **73**, 4260 (1993).
[18] J. M. Sanchez, D. Gratias, and D. de Fontaine, Acta Crystallogr. Sec. A **38**, 214 (1982).
[19] D. de Fontaine, Acta Metall. **23**, 553 (1975).
[20] E. M. Lifshitz, Fiz. Zh. **7**, 61 (1942); **7**, 251 (1942).